



Improving the Prediction Accuracy of MRI Brain Tumor Detection and Segmentation

S.T. Padmapriya¹, T.Chandrakumar¹ and T.Kalaiselvi²

¹Department of Applied Mathematics and Computational Science, Thiagarajar College of Engineering, Madurai, Tamil Nadu, India

²The Gandhigram Rural Institute (Deemed to be University), Dindigul, Tamil Nadu, India

Received 17 Apr. 2023, Revised 07 Jan. 2024, Accepted 21 Jan. 2024, Published 01 Feb. 2024

Abstract: Brain tumors were the most common kind of tumor in humans. Brain tumors can be detected from various imaging technologies. The proposed research work strives to improve the prediction accuracy of brain tumor detection and segmentation from MRI of human head scans by using a novel activation function E-Tanh. The role of activation functions is to perform computations and make decisions in artificial neural networks (ANN). We developed three ANN models for brain tumor detection by modifying the hidden layers. We have trained these ANN models using the E-Tanh activation function and evaluated their performance. This novel activation function achieved 98% prediction accuracy for the MRI brain tumor image detection neural network model, which was higher than the existing activation functions. We also have segmented brain tumors from the BraTS2020 dataset by using this activation function in U-Net-based architecture. We attained dice scores of 83%, 95%, and 85% for the whole, core, and enhancing tumors, which are significantly higher than the ReLU activation function.

Keywords: Activation Functions, Artificial Neural Networks, MRI, Brain Tumor Detection, Brain Tumor Segmentation, Accuracy, U-Net, ResNet

1. INTRODUCTION

A tumor is defined as the unrestrained proliferation of cancer cells in any region of the human body [1]. Brain tumors are split into two categories namely the benign tumor and the malignant brain tumor. Here, a benign tumor normally develops in the inner segment of the brain and do not spread across the body. However, a malignant tumor is capable of getting developed to any parts of the body and may also reach out to the brain effortlessly. For a patient, the Magnetic Resonance Imaging (MRI) generates a larger number of scans which are required to be processed by the medical consultants manually in a shorter period of time. As a consequence, the automated segmentation procedure has gained importance while processing these scans. Tumor segmentation in the brain is the process of separating aberrant cells from normal brain tissues such as necrotic core, active cells, and edema [2]. Brain segmentation methods make it simple to identify abnormal brain tumor tissues. It should be observed that these approaches are yet to produce more accurate results [3].

The Artificial neural networks (ANN) are grounded on the functionality of the human brain. The ANN's employs training examples to gain knowledge about the patterns

and the relationships hidden in the chosen dataset [4]. The structure of the ANN is influenced by information that flows through the network because a neural network learns based on that input and output. One of the critical components of neural networks is the activation functions. A neural network model's computational efficiency and training or testing accuracy is relying upon its activation function. The activation function brings a nonlinear property to the neural network so as to formulate a more accurate detection problem [5] by modifying the learned patterns.

The ANNs forms the foundation of deep neural networks, which consists of huge hidden layers. A multilevel representation learning strategy that allows the transformation of simple nonlinear modules from input to higher abstractions are referred to as Deep Learning Algorithms. The constraint such as hyperparameters optimization of traditional learning algorithms motivates the researchers to apply deep learning techniques for getting better results [6].

Previous research [7], [8], has used logistic sigmoid activation functions in neural networks, although they rarely address saturation issues. This problem can lead to reducing the effectiveness and efficiency of the learning process [9].



To overcome this limitation, developing a novel activation function could prove fruitful [10]. Therefore, in this research, we intend to design a similar activation function, namely E-Tanh, for image processing ANN models. In a previous research paper by the first author [11], E-Tanh was developed and tested on standard image recognition datasets such as MNIST, CIFAR10 and CIFAR100. However, in this proposed research, we apply the E-Tanh for MRI detection and segmentation of brain tumors. The necessary experiments were performed using the MRI scans of brain volumes acquired from the Brats2020 brain tumor detection and segmentation repository. The recognition accuracy was measured and compared to similar models where the calculations are controlled by the traditional activation functions. It is observed that E-Tanh performs better compared to the existing activation functions such as ReLU, Sigmoid, Tanh, Swish and E-Swish. Brain tumor segmentation was also performed using E-Tanh and was observed to perform well compared to the ReLU activation function [12].

Section 2 describes the related works in the literature on brain tumor detection and segmentation. The description of activation functions have been explained in Section 3. In Section 4, the explanation of E-Tanh activation function is provided. Section 5 describes the materials and metrics used in our experiments. Section 6 presents our proposed approach (methodology) and its working principle. The experimental results and our discussions on it are presented in Section 7. Section 8 concludes our research work followed by scope for future research works.

2. RELATED WORKS

The Deep Learning has gained significant importance among the researchers to process unstructured data. The Deep learning is also nowadays found widely used in the biomedical research. Specifically, the segmentation of brain tumors is well supported by the application of Convolutional Neural Networks (CNN), a component of Deep Learning [13]. While the CNN learns the differentiating characteristics from the input data, conventional and machine learning segmentation approaches feed their systems with hand-crafted image features [14], [15], [16]. Instead of extracting features, the foundation of deep learning research includes network architecture design. The CNN typically uses the patches that are extracted from images as inputs. To extract more complicated features from the data, it applies sub-sampling and trainable convolutional filters.

The most recent deep learning technique is multimodal MRI brain tumor segmentation [17]. All the MRI imaging modalities, including T1, T1c, T2, and FLAIR, are used to extract the patches. The CNN's receives this combined input of these patches or cubic voxels. For multimodal MRI glioma, a three-dimensional CNN architecture was suggested by a previous research [18]. Raju et al. (2018) [19] created an interpretation technique by employing two-dimensional CNN structures as an alternative to this method. This helps us to handle high-dimensional CNN

structures. In all these research studies, the Deep Learning Architectures uses the ReLU as the activation function.

Cascaded two pathway CNN architecture employing Nvidia GPU was proposed as a unique method for segmenting brain tumors by Havaei et al. (2017). This two-dimensional technique removes both small and large areas simultaneously. It is suggested to use a similar methodology that was used to build two pathway approaches utilizing a single CNN [20]. Using smaller 3 x 3 filters and deeper designs, several writers have suggested segmenting brain tumors [21]. They have concluded that smaller kernels yield more accurate results than larger ones. Here, a nonlinear activation function is created using the leaky rectified linear unit.

An ensemble technique that combines CNN with clustering strategies was used [17]. For segmenting brain tumors, this technique combines CNN and local structure prediction. Ground truth images are used to extract the voxels of image patches, which are thereafter grouped using the k-means algorithm. Later, the multi-modal input picture patches are classified into three clusters using a two-dimensional CNN. A different technique separates the input patches from the four different modalities of MRI [22]. Four distinct CNNs were used to process these patches, and the results of these four CNNs are combined and used as feature map for a random forest classifier using a graphical processing unit [23].

In one of the previous research studies, the first author has proposed an automated segmentation of the substructures of brain tumors using brain MRI [3]. To extract tumor substructures, a Deep Learning Model was developed by integrating the U-Net and ResNet architectures. This architecture was trained using the ReLU activation function. However, this prior research work did not deal with the issue of finding the exact borders of the tumor region since all negative values are zeroed out by ReLU. Hence, in this research work, we address this issue by proposing an activation function "E-Tanh" by including the very negative values which are most important to locate the exact location of the brain tumor. According to the authors [14], [15], [16], a method for acquiring numerous images of brain tumor tissues using fluorescence microscopy, stimulated Raman scattering microscopy and second harmonic imaging was developed. These images capture various facets of the tissue, including tissue structure, protein expression, and cell shape. After analyzing these images using deep learning algorithms, the study classified brain tumors into different groups based on their molecular and genetic characteristics. Using a collection of brain tumor images with known molecular and genetic characteristics, the deep learning algorithms learned to recognize specific features and patterns associated with different tumor types. [16] described a method for classifying MR images of the brain into multiple groups based on the presence or absence of glioma tumors by extracting features from pre-trained

CNNs trained on huge image datasets. The technique takes into account the 3D structure of the MRI images as well as the texture and intensity properties of the image voxels. Using a large dataset of sites known to harbour glioma tumors, the study evaluated the algorithm's performance and compared its results to those of other available tumor detection and classification techniques. The results showed that their method performed better than the other methods in detecting and classifying glioma tumors from the images. In a work by [14], the authors describe a method for extracting high-level features from MRI scans using pre-trained DNN models, followed by using a Support Vector Machine (SVM) classifier to classify the images according to the presence or the Presence to be divided into groups Absence of glioma tumors. The technique combines a variety of image processing algorithms to pre-process the MRI images before feature extraction, taking into account both their 2D and 3D properties. Using a data set that includes sites known to harbour glioma tumors, the study evaluated the performance of the algorithm and compared its results to those of other available tumor detection and classification techniques. The results showed that their method outperforms other approaches in accurately and sensitively identifying and classifying glioma tumors from the images. Depending on the presence or absence of tumors, the authors proposed a method to classify brain MRI images into different groups using dark nets, a form of deep convolutional neural network (CNN) [15]. The procedure also involves segmenting the MRI images of the brain into smaller, easier-to-handle sections for examination using the super pixel technique. Using a dataset of brain MRI scans with known tumor areas; the study evaluated the performance of the algorithm and compared its results with those of other available methods for tumor detection and classification. The results showed that their method performed better than the other methods in identifying and classifying brain tumors from the images.

A. Research Gap

Based on our discussion on the previous section and specifically, from the existing works [17], [21], [20], [19], [3], [11], [24], it is evident that the brain tumor detection and the segmentation architectures were trained using the ReLU. The limitation on using the ReLU activation is that it replaces all the negative values with zero. While processing the medical images, every element of MRI scans should be preserved and considered equally important so as to improve the accuracy of the prediction. For instance, very negative values should be preserved to locate the exact borders of the tumor region. Thus, a novel activation function "E-Tanh" that preserves the very negative values was employed in this research work to improve the accuracy rate of the prediction in detecting and segmenting the brain tumors.

We now state our research objective as improving the prediction accuracy of detection and segmentation of brain tumor from MRI of human head scans. We strive to meet

this objective by using the E-Tanh activation function which is described in the next section.

3. DESCRIPTION OF ACTIVATION FUNCTIONS

The activation function in neural networks computes the sum of biases and inputs. It often uses gradient processing techniques to process data and generates output for neural networks. Depending on the function it represents, the activation function can be specified as either a linear or a nonlinear function. It may be used for a variety of applications, including object recognition and categorization [25], [26], voice recognition [27], segmentation [11], scenario comprehension and description [28][29], machine translation [30], speech systems [31], cancer diagnosis [32], [33], biometrics [34], and weather forecasting [35].

A linear model maps an input function to an output function linearly. This is done in the hidden layers before making the predictions. The transformation of input vector x is given by

$$f(x) = w^T x + b \quad (1)$$

Where the input is denoted by x , weight is denoted by w , and b refers to biases.

In order to convert the linear outputs into nonlinear outputs for further processing, activation functions are required. It helps to learn the patterns in data. The output is represented by

$$y = w_1x_1 + w_2x_2 + w_3x_3 + \dots + w_nx_n + b \quad (2)$$

This output is fed into the next hidden layer for deep neural networks until the final output is obtained. The nonlinear output after applying the activation function is given by

$$y = \alpha(w_1x_1 + w_2x_2 + w_3x_3 + \dots + w_nx_n + b) \quad (3)$$

Where α is the activation function.

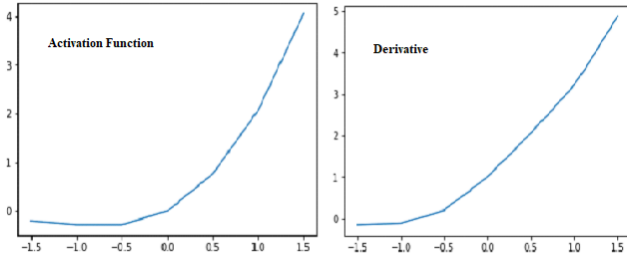
4. DESIGN AND DERIVATION OF E-TANH

The E-Tanh function is derived by extending the hyperbolic tangent function. The E-Tanh function has a small slope for very negative values. The plot of E-Tanh and its derivative are depicted in Figure 1. Figure 1 shows that there is a small slope for very negative values. The equation of the E-Tanh function is given by

$$f(x) = \alpha * e^x * Tanh(x) \quad (4)$$

The derivative of (4) is given by

$$f^1(x) = \alpha * e^x(Tanh(x) - Tanh^2(x) + 1) \quad (5)$$

Figure 1. Plot of E-Tanh and its derivative when $\alpha=1$

The non-monotonic, smoothness, limited below, and unbounded above characteristics of the E-Tanh activation function make it suitable to other activation functions such as ReLU, Sigmoid, Tanh, Swish and E-Swish. The E-Tanh gets sparsity as in ReLU due to its property of bounded below. The Negative values are allocated to zero. Because the outputs are not saturated to the maximum value for very big numbers, the E-Tanh has never been bounded above. A smooth curve denotes the smoothness of the output landscape. When optimizing the model, the smoothness property will be of greater advantage while converging the model towards minimum loss. When the gradients are near zero, the unboundedness property is suitable while the training becomes slow to prevent saturation. The plot of all the other activation functions such as Mish, ReLU, Tanh, Sigmoid, LeakyReLU, Softplus and Swish are shown in Figure 2 (www.towardsdatascience.com).

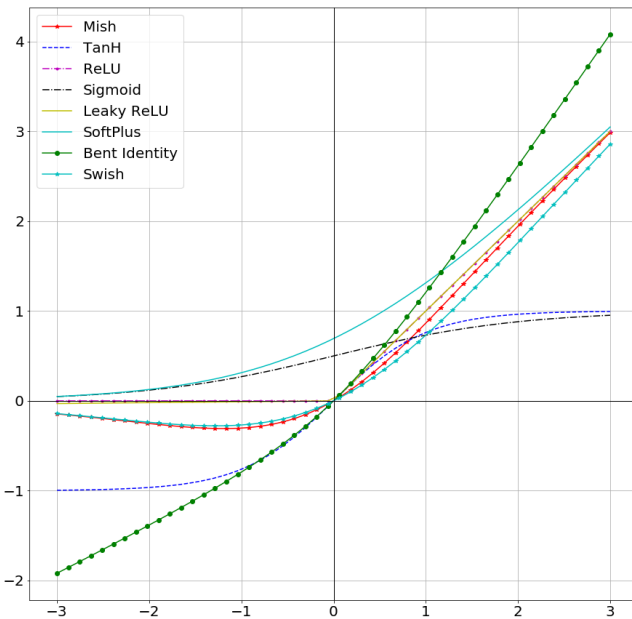


Figure 2. A plot of all Activation Functions

5. MATERIALS AND METRICS

The dataset and the system configuration required for carrying out the experiments for this research work is

discussed in this section. For detecting and segmenting brain tumors, we used the BraTS2020 dataset, which has 305 volumes of training pictures. There were 290 volumes utilized for training and 15 volumes used for prediction. The test is run on a 64-bit i3 CPU with two GB of RAM. In order to carry out our tests, we employed the Python packages namely the Keras and the TensorFlow.

The metrics employed in our experiments are as follows.

$$\text{Accuracy} = \frac{TP + TN}{TP + TN + FP + FN} \quad (6)$$

$$\text{Recall} = \frac{TP}{TP + FN} \quad (7)$$

$$\text{True Negative Rate} = \frac{TN}{TN + FP} \quad (8)$$

$$\text{Positive Predictive Rate} = \frac{TP}{TP + FP} \quad (9)$$

$$\text{Dice Coefficient / F Measure} = \frac{2 * \text{Precision} * \text{Recall}}{\text{Precision} + \text{Recall}} \quad (10)$$

The number of well recognized tumor images is denoted by TP. The number of normal images recognized exactly is denoted by TN. The FP is the number of tumor images that were incorrectly recognized. The FN is the number of normal images that were incorrectly recognized.

6. METHODOLOGY

The proposed method was carried out using BraTS2020 datasets. A high-level view of the proposed work's methodology is shown in Figure 3. Initially, the tumor and non-tumor slices were provided as inputs to the brain tumor detection models. These models will detect the slices with tumor and sends them as input to the brain tumor segmentation model. This model will segment the tumor and its substructures which enables the medical consultants to trace the tumor region.

The BraTS 2020 dataset comprises of 305 preoperative multimodal scan volumes. There are 239 HGG volumes and 66 LGG volumes among them. Four modalities of brain MRI are combined into a single volume. Each tumor was categorized as edema, necrosis, enhancing, or non-enhancing. To begin, normalize each slice of training data in all modalities except ground truth images. Each MRI image modality was thereafter normalized.

A. Brain Tumor Detection

The experiment is carried out on three types of ANN models for classifying abnormal slices from MRI of human head scans. These ANN models are developed by varying the number of hidden layers. Here, the ANN with two hidden layers are labelled as TANN, and the ANN with four and six hidden layers are labelled as FANN and SANN respectively. Figure 4 shows the architecture of TANN model. Figure 5 shows the architecture of FANN model. Figure 6 shows the architecture of SANN model.

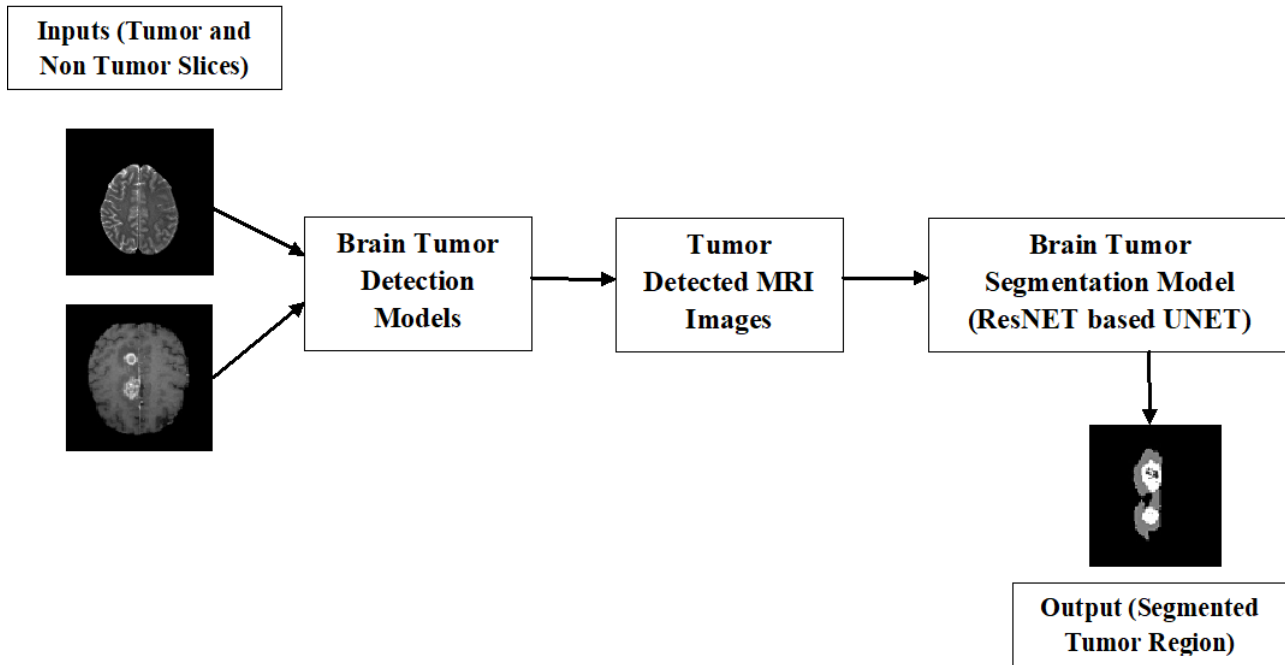


Figure 3. Methodology of the Proposed Work

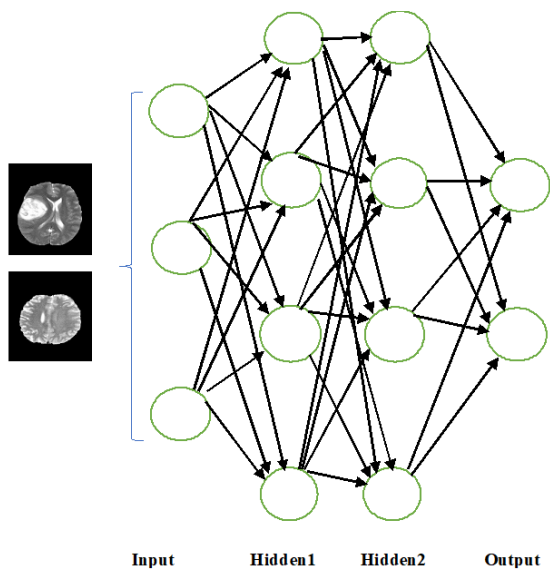


Figure 4. TANN Architecture

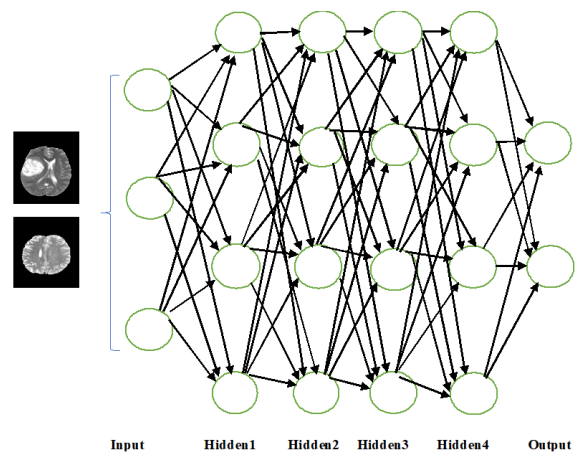


Figure 5. FANN Architecture

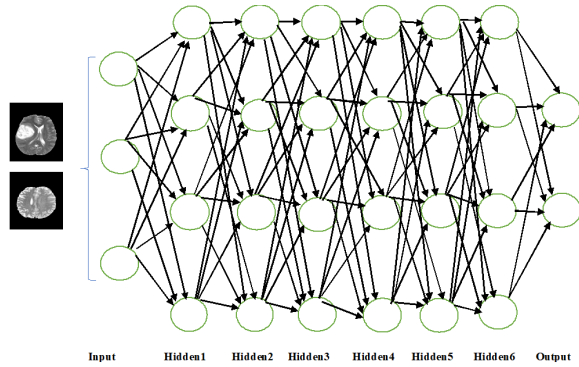


Figure 6. SANN Architecture

B. Brain Tumor Segmentation

The ResNet-based UNET architecture is used for segmenting brain tumors from MRI of human brain scans. The Patch-based segmentation technique [36] is used to segment the brain tumors. The proposed architecture will be trained using patches generated from MRI volumes. To remove the class variation problem in the data, the collected patches were subjected to data augmentation methods. The data augmentation procedures include tilting, scaling, horizontal flips, and duplicating the acquired patches. Figure 7 depicts the proposed segmentation model's architecture.

The proposed network was trained utilizing patches derived from axial MRI slices of high and low-grade glioma patients, as well as the matching ground truth [36]. To minimize the loss function and eliminate the class variance problem, we used weighted cross-entropy (WCE) and generalized dice loss (GDL). The following are the definitions of the WCE and GDL:

$$WCE = -\frac{1}{b} \sum_j \sum_i^L W_i g_{ij} \log(p_{jk}) \quad (11)$$

$$GDL = \frac{1 - 2 \sum_i^L W_i \sum_j g_{ij} P_{ij}}{\sum_i^L W_i \sum_j (g_{ij} + P_{ij})} \quad (12)$$

$$\text{Where, } W_i = \frac{1}{(\sum_j g_{ij})^2} \quad (13)$$

Where L – Total number of labels,

k - batch size,

W_i - weight,

P_{ij} - ith and jth pixel values of the segmented binary image,

g_{ij} - ith and jth pixel values of the binary ground truth.

The trained model is stored, and a prediction is made using that model. Then, four MRI modalities that have never been trained previously were used as input for evaluation. Finally, the segmented image will be retrieved by the trained model.

7. RESULTS AND DISCUSSIONS

A. Brain Tumor Detection

We have used ReLU, sigmoid, Tanh, Swish, E-Swish, and E-Tanh for training the ANN models and compared the training accuracy of these activation functions. The TANN model was at first trained for 30 epochs, and the obtained accuracy results are shown in Table II. The training accuracy of ReLU for this neural network model is 88%. The accuracy of the sigmoid is 79.21%. The training accuracy of the Tanh activation function is 85%. The accuracy for swish and e-swish activation functions is 82% and 84% respectively. The accuracy of the proposed function is 94% when the value of alpha is 1. At the same time, the existing functions' accuracy results are lesser than 90%. The values of recall, true negative rate, positive predictive value and F Measure for all the activation functions are shown in Table I.

TABLE I. Experimental Results of Activation function's Test Accuracy in TANN with $\alpha=1$

S.NO	AF	Accuracy (%)	Recall	True Negative Rate	Positive Predictive Value	F Measure
1	ReLU	88	72	94	82	76
2	Sigmoid	79	52	87	58	54
3	Tanh	85	65	92	76	76
4	Swish	82	58	90	69	63
5	E-Swish	84	62	91	73	67
6	E-Tanh	94	84	96	88	85

The accuracy of E-Tanh function was verified and validated by varying the value of alpha. The obtained results are shown in Table II. We have varied the alpha value from 0.5 to 1.75 ($0.5 \leq \alpha \leq 1.75$) and have recorded the percentage of accuracy. Within this interval, the accuracy increases. When the value of alpha is 0.5, the accuracy is 90%. Moreover, the accuracy was constantly increasing till the value of alpha reaches 1.75. We got an accuracy of 98% when the value of alpha is 1.75. When the value of alpha is set to 2, then the accuracy is found decreasing gradually. Thus, we observe that when the alpha value is within 0.5 and 1.75, it produces an exceptional accuracy. The plot of E-Tanh and its derivative when $\alpha = 1.75$ is shown in Figure 8. We have attained the best accuracy when the value of alpha is set to 1.75. Hence, the FANN model and SANN model

TABLE II. Accuracy obtained by varying the value of α in E-Tanh

S.NO	Value of Alpha	Accuracy (%)	Recall	True Negative Rate	Positive Predictive Value	F Measure
1	0.5	90	90	95	85	87
2	1	94	93	96	88	90
3	1.25	95	95	97	90	92
4	1.5	96.5	96	97	92	93
5	1.75	97.9	97	98	95	95
6	2	96	96	97	92	93

were trained using the E-Tanh function with an alpha value of 1.75.

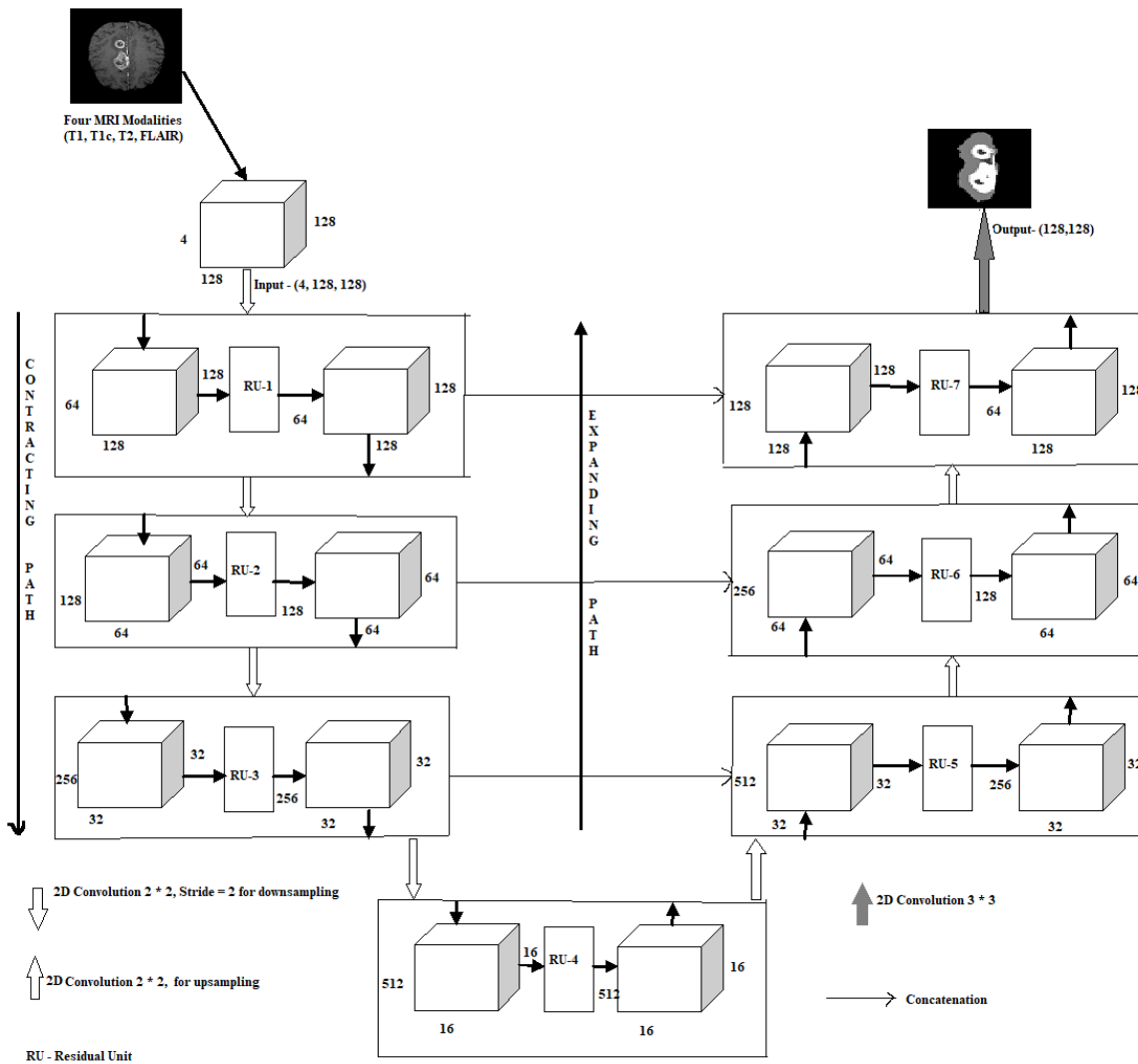


Figure 7. Brain Tumor Segmentation Architecture

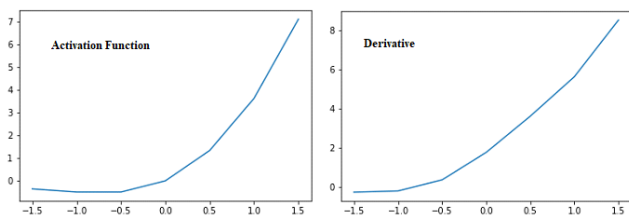


Figure 8. E-Tanh and it's derivative when $\alpha = 1.75$

TABLE III. Experimental Results of Activation function's Test Accuracy in FANN

S.NO	AF	Accuracy (%)	Recall	True Negative Rate	Positive Predictive Value	F Measure
1	Relu	97	96	97	92	93
2	Sigmoid	97	96	97	92	93
3	Tanh	96	96	97	92	93
4	Swish	97.3	97	98	95	95
5	E-Swish	98	98	99	96	96
6	E-Tanh($\alpha = 1.75$)	97.8	97	98	96	96

The FANN model was trained using different activation functions. Their accuracy, recall, true negative rate, positive predictive value, and F Measure values are shown in Table III.

The SANN model was trained using different activation functions. Their accuracy, recall, true negative rate, positive predictive value, and F Measure values are shown in Table IV.

TABLE IV. Experimental Results of Activation function's Test Accuracy in SANN

S.NO	AF	Accuracy (%)	Recall	True Negative Rate	Positive Predictive Value	F Measure
1	Relu	97	96	97	92	93
2	Sigmoid	96.3	96	95	92	93
3	Tanh	95.7	95	96	91	93
4	Swish	97	96	97	92	93
5	E-Swish	97	96	97	92	93
6	E-Tanh($\alpha=1.75$)	98	98	99	96	96

B. Brain Tumor Segmentation

We have trained and validated our segmentation model using BraTS 2020 training/testing image datasets in the proposed work. We have performed similarity checks using various prominent assessment metrics. We began by training the segmentation model with ReLU. In the residual units, we employed the PReLU activation. The model was evaluated using the dice score (DS), recall (SEN), and true negative rate (SPE) metrics, and the results are shown in Table VI. The segmentation model was trained from the scratch, with the basic U-Net block utilizing E-Tanh and residual block using the PReLU AF. Table V illustrates the findings of the trained model's evaluation using test set. The segmented brain tumor substructures obtained by ReLU are shown in Figure 9. The segmented brain tumor substructures obtained by E-Tanh function are shown in Figure 10.

TABLE V. Experimental Results of Activation function's Test Accuracy in SANN

S.NO	BRAIN TUMOR SUBSTRUCTURES	RELU ACTIVATION	E-TANH ACTIVATION
1	Whole tumor	DS	81
		SEN	97
		SPE	99
2	Core Tumor	DS	93
		SEN	97
		SPE	99
3	Enhancing Tumor	DS	83
		SEN	92
		SPE	99

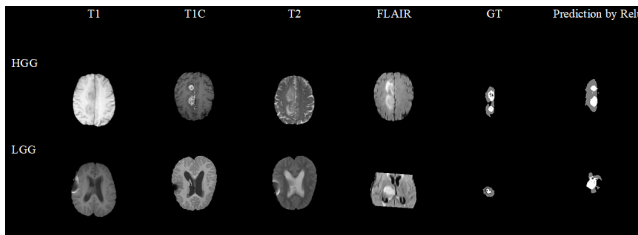


Figure 9. Segmentation Results of ReLU

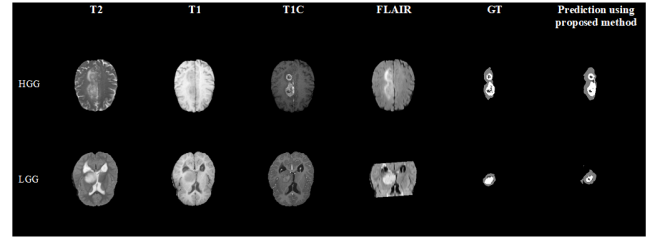


Figure 10. Segmentation Results of E-Tanh

The proposed segmentation methods were compared against the existing approaches that employ Deep Learning on the BraTS dataset. We received the best dice value for core tumors using these segmentation approaches. When compared to other approaches such as generative adversarial networks (GAN's) [37], mixed supervision [38], dual force CNN [39], integration of FCNN's and CRF's [40], the dice score of complete and improved tumor is competitive. Table VI summarizes the findings of the comparison of dice scores with other methods in the literature.

TABLE VI. Performance Comparison of Proposed Method with Existing Methods

Author& Year	Dice Coefficient		
	Whole Tumor	Core Tumor	Enhanced Tumor
Nema et.al. 2020 [37]	94.63	85.6	93.5
Mlynarski et.al. 2019 [38]	80	63	66
Wang et.al. 2019 [41]	94	-	-
Chen et.al. 2019 [39]	89	73	73
Sajid et.al. 2019 [42]	86	86	88
Zhao et.al. 2018 [40]	81	65	60
Hussain et.al. 2018 [43]	86	87	90
Pereira et.al. 2016 [21]	88	83	77
Havaei et.al. 2016 [20]	88	79	73
Kalaiselvi et.al.2022 [3]	81	93	83
Proposed Method	83	95	85

Table VII indicates the performance of the proposed method compared to the existing techniques that uses BraTS2020 for brain tumor segmentation.

TABLE VII. Performance Comparison of Proposed Method with the State-of-the-art Methods

Author& Year	Dice Coefficient		
	Whole Tumor	Core Tumor	Enhanced Tumor
Kalaiselvi et.al. 2022 [11]	81	93	83
Henry et al., 2020 [44]	88	84	78
Proposed Method	83	95	85

The detection accuracy of TANN model is shown in Table I. It is evident that the E-Tanh activation function produces better results when compared to the other activation functions. From Table III, it is visible that the e-swish activation performs much better when compared to all other activation functions. The E-Tanh function performs

well when compared with other activation functions. From Table IV, it can be seen that E-Tanh performed well in ANN with six hidden layers when compared to all other activation functions.

From Table V, it can be seen that the model architecture that was trained with E-Tanh showed better results when compared to the model architecture that is trained with the ReLU activation. Due to the property of preserving very negative values, the E-Tanh could locate the borders of the tumor portion very effectively when compared to the ReLU activation function.

The accuracy of brain tumor detection using the E-Tanh function sounds better than the predictions by other activation functions as evidenced from the Figure 11. When compared with ReLU, the E-Tanh function provides a better dice score for brain tumor segmentation. It is shown in Figure 12.

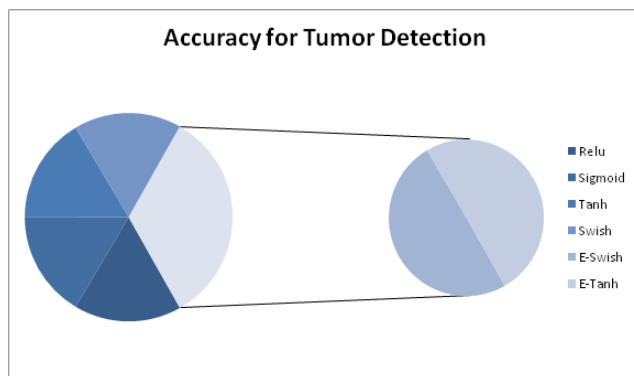


Figure 11. Improvement of Tumor Detection Accuracy using E-Tanh

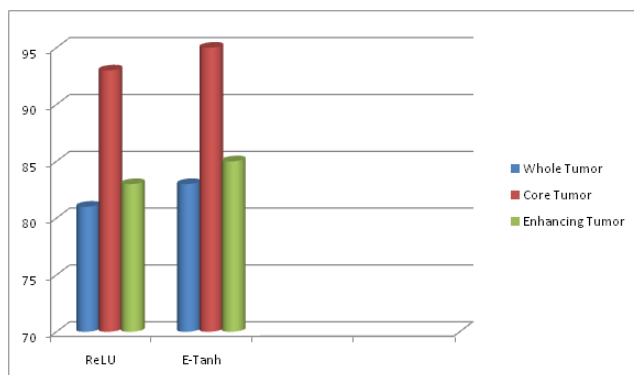


Figure 12. Performance of ReLU and E-Tanh in Brain Tumor Segmentation

8. CONCLUSIONS AND SCOPE FOR FUTURE RESEARCH

In this research work, we have used a neural network activation function “E-Tanh” for neural network models. We understand that the E-Tanh function outperforms other well-known activation functions by attaining accuracy of 98% in

brain tumor detection. In brain tumor segmentation, it shows promising results when compared to the ReLU activation function. Our contribution to the theory of research in brain tumor segmentation is the development of a novel neural network activation function ‘E-Tanh’ for medical images. There are many such activation functions in the literature to train neural networks.

Among them, the Rectified Linear Unit (ReLU) is widely used to train image datasets because of its sparsity. However, our research focuses on analyzing medical images with improved prediction accuracy. It is observed that the ReLU eliminates all the negative values and makes it as zero where some important details of the images cannot be trained to the neural networks. However, in our proposed method, the E-Tanh function allows some negative values where some minute details of the images are trained to the neural networks. This activation function is developed for medical image detection and segmentation. We have experimented with E-Tanh function in classifying and segmenting brain tumors which gave promising results. We suggest that the E-Tanh function could be used in brain tumor detection and segmentation as it poses a positive climate for its utilization in practice. In the instance of a whole and enhancing tumor, the proposed segmentation approach did not yield a high dice score. In future, the segmentation model architecture will be fine-tuned to achieve better outcomes in segmenting whole and enhancing tumors. In our future research, the E-Tanh activation function will be applied for training deep neural network models for medical image analysis.

REFERENCES

- [1] T. Kalaiselvi, S. Padmapriya, P. Sriramakrishnan, and K. Somasundaram, “A deep learning approach for brain tumour detection system using convolutional neural networks,” *International Journal of Dynamical Systems and Differential Equations*, vol. 11, no. 5-6, pp. 514–526, 2021.
- [2] S. Banerjee, S. Mitra, and B. U. Shankar, “Automated 3d segmentation of brain tumor using visual saliency,” *Information Sciences*, vol. 424, pp. 337–353, 2018.
- [3] T. Kalaiselvi and S. Padmapriya, “Multimodal mri brain tumor segmentation—a resnet-based u-net approach,” in *Brain Tumor MRI Image Segmentation Using Deep Learning Techniques*. Academic Press, 2022, pp. 123–135.
- [4] Y. LeCun, Y. Bengio, and G. Hinton, “Deep learning,” *nature*, vol. 521, no. 7553, pp. 436–444, 2015.
- [5] M. Manavazhahan, “A study of activation functions for neural networks,” *MICCAI Multimodal Brain Tumor Segmentation Challenge*, pp. 31–35, 2017.
- [6] N. Jones, “Computer science: The learning machines,” *Nature News*, vol. 505, no. 7482, p. 146, 2014.
- [7] P. Ramachandran, B. Zoph, and Q. V. Le, “Swish: a self-gated activation function,” *arXiv preprint arXiv:1710.05941*, vol. 7, no. 1, 2017.



- [8] M. A. Mercioni and S. Holban, "P-swish: Activation function with learnable parameters based on swish activation function in deep learning," in *2020 International Symposium on Electronics and Telecommunications (ISETC)*. IEEE, 2020, pp. 1–4.
- [9] I. Goodfellow, Y. Bengio, and A. Courville, *Deep learning*. MIT press, 2016.
- [10] P. Ramachandran, B. Zoph, and Q. V. Le, "Searching for activation functions," *arXiv preprint arXiv:1710.05941*, 2017.
- [11] T. Kalaiselvi, S. Padmapriya, K. Somasundaram, and S. Praveenkumar, "E-tanh: a novel activation function for image processing neural network models," *Neural Computing and Applications*, pp. 1–13, 2022.
- [12] J. Schmidt-Hieber, "Nonparametric regression using deep neural networks with relu activation function," *The Annals of Statistics*, vol. 48, no. 4, pp. 1875–1897, 2020.
- [13] G. Urban, M. Bendszus, F. Hamprecht, J. Kleesiek et al., "Multimodal brain tumor segmentation using deep convolutional neural networks," *MICCAI BraTS (brain tumor segmentation) challenge. Proceedings, winning contribution*, pp. 31–35, 2014.
- [14] G. Latif, D. A. Iskandar, J. Alghazo, and M. M. Butt, "Brain mr image classification for glioma tumor detection using deep convolutional neural network features," *Current medical imaging*, vol. 17, no. 1, pp. 56–63, 2021.
- [15] G. Latif, G. Ben Brahim, D. A. Iskandar, A. Bashar, and J. Alghazo, "Glioma tumors' classification using deep-neural-network-based features with svm classifier," *Diagnostics*, vol. 12, no. 4, p. 1018, 2022.
- [16] J. Gesperger, A. Lichtenegger, T. Roetzer, M. Salas, P. Eugui, D. J. Harper, C. W. Merkle, M. Augustin, B. Kiesel, P. A. Mercea et al., "Improved diagnostic imaging of brain tumors by multimodal microscopy and deep learning," *Cancers*, vol. 12, no. 7, p. 1806, 2020.
- [17] P. Dvořák and B. Menze, "Local structure prediction with convolutional neural networks for multimodal brain tumor segmentation," in *International MICCAI workshop on medical computer vision*. Springer, Cham, 2016, pp. 59–71.
- [18] D. Zikic, Y. Ioannou, M. Brown, and A. Criminisi, "Segmentation of brain tumor tissues with convolutional neural networks," *Proceedings MICCAI-BRATS*, no. 2014, pp. 36–39, 2014.
- [19] K. Raju and N. N. Chiplunkar, "A survey on techniques for cooperative cpu-gpu computing," *Sustainable Computing: Informatics and Systems*, vol. 19, pp. 72–85, 2018.
- [20] M. Havaei, A. Davy, D. Warde-Farley, A. Biard, A. Courville, Y. Bengio, C. Pal, P.-M. Jodoin, and H. Larochelle, "Brain tumor segmentation with deep neural networks," *Medical image analysis*, vol. 35, pp. 18–31, 2017.
- [21] S. Pereira, A. Pinto, V. Alves, and C. A. Silva, "Brain tumor segmentation using convolutional neural networks in mri images," *IEEE transactions on medical imaging*, vol. 35, no. 5, pp. 1240–1251, 2016.
- [22] V. Rao, M. S. Sarabi, and A. Jaiswal, "Brain tumor segmentation with deep learning," *MICCAI multimodal brain tumor segmentation challenge (BraTS)*, vol. 59, pp. 1–4, 2015.
- [23] A. Bal, M. Banerjee, P. Sharma, and R. Chaki, "A multi-class image classifier for assisting in tumor detection of brain using deep convolutional neural network," *Advanced Computing and Systems for Security*, pp. 93–111, 2020.
- [24] Z. Ullah, M. Usman, M. Jeon, and J. Gwak, "Cascade multiscale residual attention cnns with adaptive roi for automatic brain tumor segmentation," *Information sciences*, vol. 608, pp. 1541–1556, 2022.
- [25] S. S. Md Noor, K. Michael, S. Marshall, and J. Ren, "Hyperspectral image enhancement and mixture deep-learning classification of corneal epithelium injuries," *Sensors*, vol. 17, no. 11, p. 2644, 2017.
- [26] V. Badrinarayanan, A. Kendall, and R. Cipolla, "Segnet: A deep convolutional encoder-decoder architecture for image segmentation," *IEEE transactions on pattern analysis and machine intelligence*, vol. 39, no. 12, pp. 2481–2495, 2017.
- [27] R. Hu, P. Dollár, K. He, T. Darrell, and R. Girshick, "Learning to segment every thing," in *Proceedings of the IEEE conference on computer vision and pattern recognition*, 2018, pp. 4233–4241.
- [28] Y. Liu and J. Zhang, "Deep learning in machine translation," *Deep learning in natural language processing*, pp. 147–183, 2018.
- [29] S. Ö. Arik, M. Chrzanowski, A. Coates, G. Damos, A. Gibiansky, Y. Kang, X. Li, J. Miller, A. Ng, J. Raiman et al., "Deep voice: Real-time neural text-to-speech," in *Proceedings of the 34th International Conference on Machine Learning*, vol. 70. JMLR. org, 2017, pp. 195–204.
- [30] W. Ping, K. Peng, A. Gibiansky, S. O. Arik, A. Kannan, S. Narang, J. Raiman, and J. Miller, "Deep voice 3: Scaling text-to-speech with convolutional sequence learning," *arXiv preprint arXiv:1710.07654*, 2017.
- [31] D. Wang, A. Khosla, R. Gargeya, H. Irshad, and A. H. Beck, "Deep learning for identifying metastatic breast cancer," *arXiv preprint arXiv:1606.05718*, 2016.
- [32] L. T. Lazimul and D. Binoy, "Fingerprint liveness detection using convolutional neural network and fingerprint image enhancement," in *2017 International Conference on Energy, Communication, Data Analytics and Soft Computing (ICECDS)*. IEEE, 2017, pp. 731–735.
- [33] H. Jung and Y. Heo, "Fingerprint liveness map construction using convolutional neural network," *Electronics Letters*, vol. 54, no. 9, pp. 564–566, 2018.
- [34] A. Uçar, Y. Demir, and C. Güzeliş, "Object recognition and detection with deep learning for autonomous driving applications," *Simulation*, vol. 93, no. 9, pp. 759–769, 2017.
- [35] C. Nwankpa, W. Ijomah, A. Gachagan, and S. Marshall, "Activation functions: Comparison of trends in practice and research for deep learning," *arXiv preprint arXiv:1811.03378*, 2018.
- [36] M. Sharif, J. Amin, M. W. Nisar, M. A. Anjum, N. Muhammad, and S. A. Shad, "A unified patch based method for brain tumor detection using features fusion," *Cognitive Systems Research*, vol. 59, pp. 273–286, 2020.
- [37] S. Nema, A. Dudhane, S. Murala, and S. Naidu, "Rescuenet: An unpaired gan for brain tumor segmentation," *Biomedical Signal Processing and Control*, vol. 55, p. 101641, 2020.

- [38] P. Mlynarski, H. Delingette, A. Criminisi, and N. Ayache, "Deep learning with mixed supervision for brain tumor segmentation," *Journal of Medical Imaging*, vol. 6, no. 3, p. 034002, 2019.
- [39] S. Chen, C. Ding, and M. Liu, "Dual-force convolutional neural networks for accurate brain tumor segmentation," *Pattern Recognition*, vol. 88, pp. 90–100, 2019.
- [40] X. Zhao, Y. Wu, G. Song, Z. Li, Y. Zhang, and Y. Fan, "A deep learning model integrating fcnn and crfs for brain tumor segmentation," *Medical image analysis*, vol. 43, pp. 98–111, 2018.
- [41] Y. Wang, C. Li, T. Zhu, and J. Zhang, "Multimodal brain tumor image segmentation using wrn-ppnet," *Computerized Medical Imaging and Graphics*, vol. 75, pp. 56–65, 2019.
- [42] S. Sajid, S. Hussain, and A. Sarwar, "Brain tumor detection and segmentation in mr images using deep learning," *Arabian Journal for Science and Engineering*, vol. 44, pp. 9249–9261, 2019.
- [43] S. Hussain, S. M. Anwar, and M. Majid, "Segmentation of glioma tumors in brain using deep convolutional neural network," *Neuro-computing*, vol. 282, pp. 248–261, 2018.
- [44] T. Henry, A. Carré, M. Lrousseau, T. Estienne, C. Robert, N. Paragios, and E. Deutsch, "Brain tumor segmentation with self-ensembled, deeply-supervised 3d u-net neural networks: a brats 2020 challenge solution," in *International MICCAI Brainlesion Workshop*. Springer, Cham, 2021, pp. 327–339.



Dr. S.T.Padmapriya is currently working as Assistant Professor in Department of Applied Mathematics and Computational Sciences at Thiagarajar College of Engineering, Madurai. She received her PhD in the Department of Computer Science and Applications, Gandhigram Rural Institute-Deemed University, Gandhigram in 2022. She received her M.Phil in Computer Science (2018-2019) from Gandhigram Rural Institute-Deemed University, Gandhigram. She received her ME in Computer Science and Engineering (2011-2013) from Sethu Institute of Technology, Virudhunagar. She received her M.Sc in Software Engineering from RVS College of Engineering and Technology (2011), Dindigul. Her research focuses on Artificial Intelligence, Machine Learning, Deep Learning, Medical Image Processing, Software Engineering and Data Analytics.



Chandrakumar Thangavel is an Associate Professor in the Department of Applied Mathematics and Computational Science at Thiagarajar College of Engineering. He received his Ph.D. from Anna University specializing in Computer Science. His research interests include software engineering, Analytics, Enterprise Resource Planning (ERP), and software quality.



Kalaiselvi Thiruvankatam received her PhD from The Gandhigram Rural Institute on Medical Image Analysis in February 2010. She received her PDF from the same department in 2011. She was a recipient of DST young scientist research fellowship during 2008–2011. Her research focuses on MRI of human brain image analysis to enrich computer aided diagnostic process, telemedicine and teleradiology technologies.